

Segmentation of Brain in MRI Images Using Watershed-based Technique

Yousif Mohamed Y. Abdallah^{1,2}, Abdalrahman Hassan^{1,3,4}

¹College of Applied Medical Science, Almajmah University, Riyadh, Saudi Arabia

²Sudan University of Science and Technology, College of Medical Radiological Science, Khartoum, Sudan

³Radiology Department, Antalia Medical Center, Khartoum, Sudan

⁴Elnileen Medical Center, Khartoum, Sudan

Abstract: *This was experimental study conducted to study segmentation of brain in MRI images using edge detection and morphology filters. For brain MRI images each film scanned using digitizer scanner then treated by using image processing program (MatLab), where the segmentation was studied. The scanned image was saved in a TIFF file format to preserve the quality of the image. Brain tissue can be easily detected in MRI image if the object has sufficient contrast from the background. We use edge detection and basic morphology tools to detect a brain. The segmentation of MRI images steps using detection and morphology filters were image reading, detection Entire brain, Dilation of the image, filling interior gaps inside the image, removal connected objects on borders and smoothen the object (brain). The results of this study were that it showed an alternate method for displaying the segmented object would be to place an outline around the segmented brain. Those filters approaches can help in removal of unwanted background information and increase diagnostic information of Brain MRI.*

Keywords: Segmentation, brain, Matlab, Morphology filters.

1. Introduction

The thyroid is made up of the isthmus which overlying the 2nd and 3rd rings of the trachea, the lateral lobes which each extending from the side of the thyroid cartilage downwards to the 6th tracheal ring and an inconstant pyramidal lobe which projecting upwards from the isthmus, usually on the left side, which represents a remnant of the embryological descent of the thyroid. The thyroid gland is enclosed in the pretracheal fascia, covered by the strap muscles and overlapped by the sternocleidomastoids. The anterior jugular veins course over the isthmus. When the thyroid enlarges, the strap muscles stretch and adhere to the gland so that, at operation, they often appear to be thin layers of fascia. On the deep aspect of the thyroid lie the larynx and trachea, with the pharynx and oesophagus behind and the carotid sheath on either side. Two nerves lie in close relationship to the gland; in the groove between the trachea and oesophagus lies the recurrent laryngeal nerve and deep to the upper pole lies the external branch of the superior laryngeal nerve passing to the cricothyroid muscle [1-4].

Nuclear Medicine is the section of science that utilizes the properties of radiopharmaceuticals in order to derive clinical information of the human physiology and biochemistry. The radiopharmaceutical follows its physiological pathway and it is concentrated on specific organs and tissues for short periods of time. Then, the patient is positioned under a nuclear medicine equipment which can detect the radiation emitted by the human body resulting in images of the biodistribution of the radiopharmaceutical. In Nuclear Medicine, there are two main methods of patient imaging, the imaging with Planar Imaging, Dynamic Imaging or SPECT and the PET. During the last decade, hybrid systems have

been developed integrating the CT technique with either SPECT or PET resulting in SPECT/CT and PET/CT respectively. This chapter will concentrate on the implementation of MatLab code in gamma camera planar imaging, SPECT and SPECT/CT methods [5-7]. The gamma camera is composed of a collimator, a scintillator crystal usually made of NaI (or CsI), the photomultiplier tubes, the electronic circuits and a computer equipped with the suitable software to depict the nuclear medicine examinations. In planar imaging, the patient, having being delivered with the suitable radiopharmaceutical, is sited under the gamma camera head. The gamma camera head remains stable at a fixed position over the patient for a certain period of time, acquiring counts (disintegrations). These will constitute the radiopharmaceutical distribution image. The counts measured in a specific planar projection originate from the whole thickness of patient [8-9]. In SPECT, the gamma camera head rotates around the patient remaining at well-defined angles and acquiring counts for specific periods of time per angle. What makes SPECT a valuable tool in nuclear medicine is the fact that information in the three dimensions of the patient can be collected in a number of slices with a finite known volume (in voxels). Thus SPECT technique is used to display the radiopharmaceutical distribution in a single slice removing the contribution from the overlying and underlying tissues. In order to obtain the most accurate quantitative data from SPECT images, two issues that have to be resolved are the attenuation correction and the Compton scattering that the photons are undergone until reach and interact with the slice of interest tissues. As an examining organ has certain dimensions, each slice along the axis of the gamma camera has different distance from the detector. Thus, each photon experiences different attenuation. These two phenomena usually lead to distortion of the measured activity concentration [10-11].

Volume 4 Issue 1, January 2015

www.ijsr.net

2. Methods and Materials

Separating touching objects in an image is one of the more difficult image processing operations. The watershed transform is often applied to this problem. The watershed transform finds "catchment basins" and "watershed ridge lines" in an image by treating it as a surface where light pixels are high and dark pixels are low. Segmentation using the watershed transform works well if one can identify, or "mark," foreground objects and background locations. Marker-controlled watershed segmentation follows this basic procedure:

1. Computation a segmentation function. This is an image whose dark regions are the objects we were trying to segment.
2. Computation the foreground markers. These are connected blobs of pixels within each of the objects.
3. Computation the background markers. These are pixels that are not part of any object.
4. Modification of the segmentation function so that it only has minima at the foreground and background marker locations.
5. Compute the watershed transform of the modified segmentation function.

Steps of brain segmentation using Matlab program:

- Step 1: The Color Image and Convert it to Grayscale Reading
- Step 2: Use the Gradient Magnitude as the Segmentation Function
- Step 3: Mark the Foreground Objects
- Step 4: Compute Background Markers
- Step 5: Compute the Watershed Transform of the Segmentation Function.
- Step 6: Visualize the Result

3. The Results

This experimental study was conducted to study an accurate liver segmentation method using a parallel computing algorithm. The sample of study was included 50 patients. The main objective of this research was.

Experimental Study

Step 1: the Color Image and Convert it to Grayscale Reading as shown in figure 1.

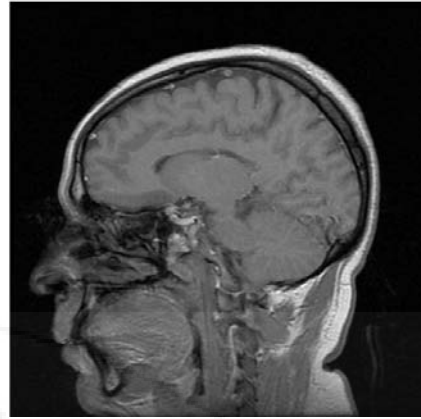


Figure 1: Shows the original image

Step 2: Use the Gradient Magnitude as the Segmentation Function

The Sobel edge masks, *imfilter*, and some simple arithmetic were used to compute the gradient magnitude. The gradient is high at the borders of the objects and low (mostly) inside the objects as shown in figure 2.

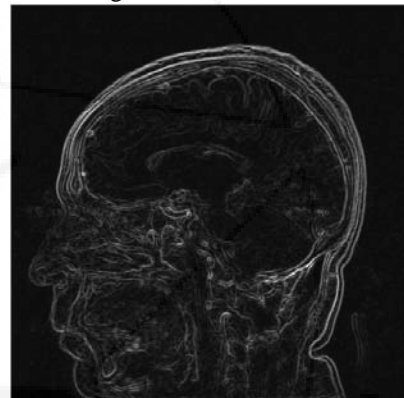


Figure 2: Gradient Magnitude as the Segmentation Function

The image was segmented by using the watershed transform directly on the gradient magnitude as shown in figure 3.

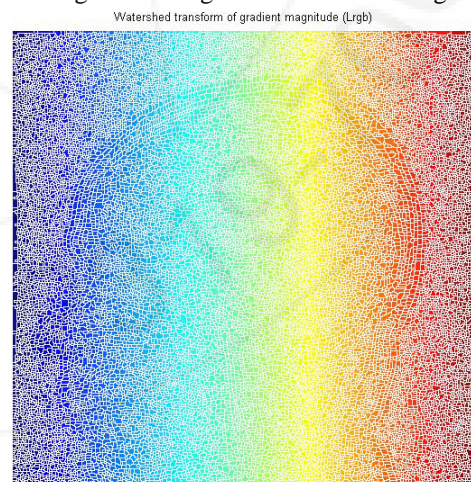


Figure 3: The watershed transform

Step 3: Mark the Foreground Objects

A variety of procedures could be applied here to find the foreground markers, which must be connected blobs of pixels inside each of the foreground objects. In this study

morphological techniques were used and they called "opening-by-reconstruction" and "closing-by-reconstruction" to "clean" up the image. These operations will create flat maxima inside each object that can be located using *imregionalmax*. Opening is an erosion followed by a dilation, while opening-by-reconstruction is an erosion followed by a morphological reconstruction as shown in figure 4.



Figure 4: The Opening-by-reconstruction algorithm

Next the opening-by-reconstruction was computed using *imrode* and *imreconstruct* as shown in figure 5.

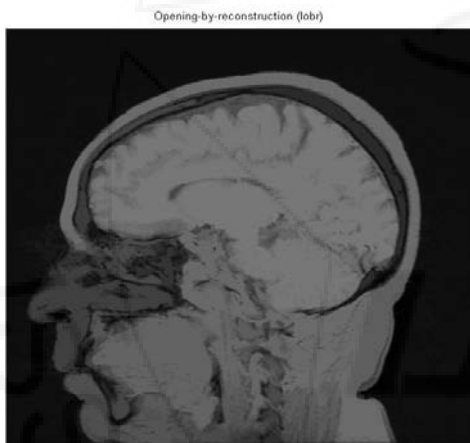


Figure 5: The opening-by-reconstruction

Following the opening with a closing can remove the dark spots and stem marks. Compare a regular morphological closing with a closing-by-reconstruction. First *imclose* code was tried as shown in figure 6.



Figure 5: The 'Opening-closing algorithm

The *imdilata* code was used followed by *imreconstruct*. The image inputs and output of *imreconstruct* should complement as shown in figure 6.

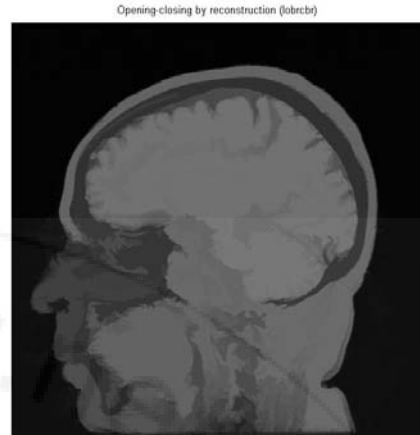


Figure 6: Opening-closing by reconstruction algorithm

When *Iobrcbr* with *Ioc* were compared, reconstruction-based opening and closing found more effective than standard opening and closing at removing small blemishes without affecting the overall shapes of the objects. Calculate the regional maxima of *Iobrcbr* to obtain good foreground markers as shown in figure 7.

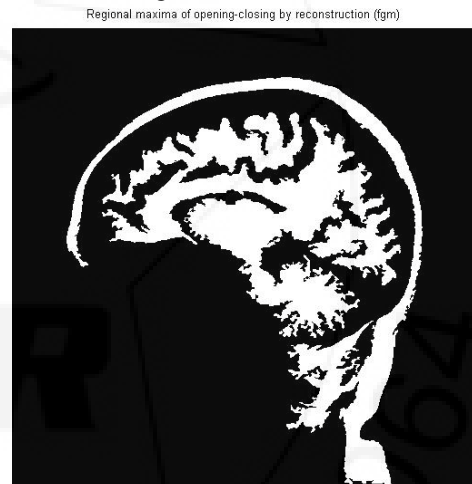


Figure 7: Regional maxima of opening-closing

To help interpret the result, superimpose the foreground marker image on the original image as shown in figure 8.

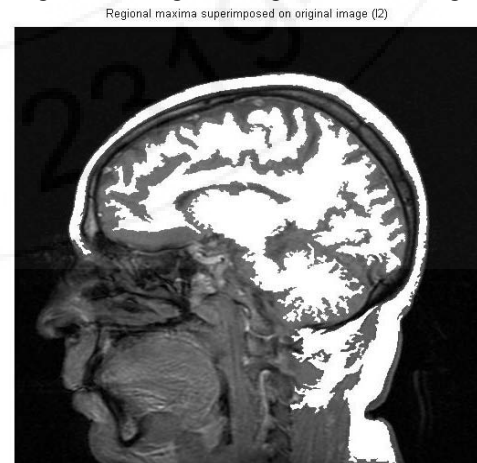


Figure 9: Regional maxima superimposed technique on original image

Some of the mostly-occluded and shadowed objects are not marked, which means that these objects will not be segmented properly in the end result. Also, the foreground markers in some objects go right up to the objects' edge. The edges of the marker blobs should clean and then shrink them a bit. This could be done by a closing followed by an erosion.

This procedure tended to leave some stray isolated pixels that must be removed. This could be done using `bwareaopen`, which removed all blobs that had less than a certain number of pixels as shown in figure 10.

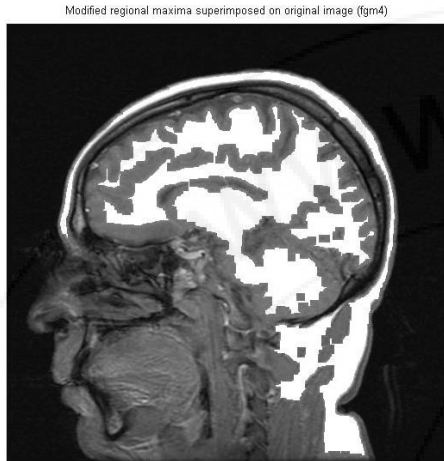


Figure 10: Modified regional maxima superimposed on original image

Step 4: Compute Background Markers

Now the background need to be marked. In the cleaned-up image, `Iobrchr`, the dark pixels belong to the background, a thresholding operation could start with as shown in figure 11.

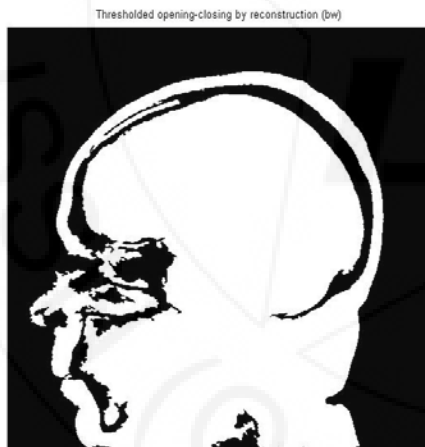


Figure 11: Thresholded opening-closing by reconstruction

The background pixels are in black, but ideally the background markers shouldn't be too close to the edges of the objects which would segment. the background would "thin" by computing the "skeleton by influence zones", or SKIZ, of the foreground of `bw`. This can be done by computing the watershed transform of the distance transform of `bw`, and then looking for the watershed ridge lines (`DL == 0`) of the result.

Step 5: Compute the Watershed Transform of the Segmentation Function.

The function `imimposemin` can be used to modify an image so that it has regional minima only in certain desired

locations. Here `imimposemin` used to modify the gradient magnitude image so that its only regional minima occur at foreground and background marker pixels. Finally we are ready to compute the watershed-based segmentation.

Step 6: The Result Visualization

One visualization technique is to superimpose the foreground markers, background markers, and segmented object boundaries on the original image. Dilation could use as needed to make certain aspects, such as the object boundaries, more visible. Object boundaries are located where `L == 0` as shown in figure 12 and figure 13a & b.

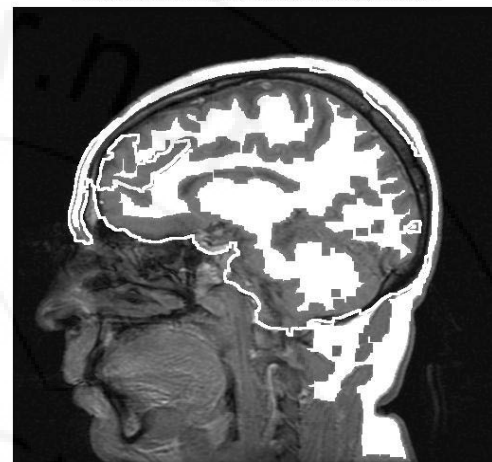


Figure 12: Markers and object boundaries superimposed on original image

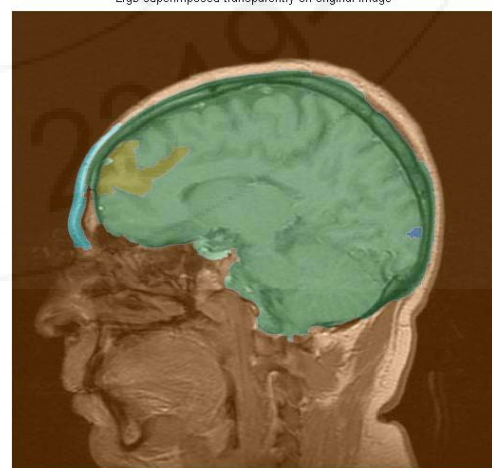
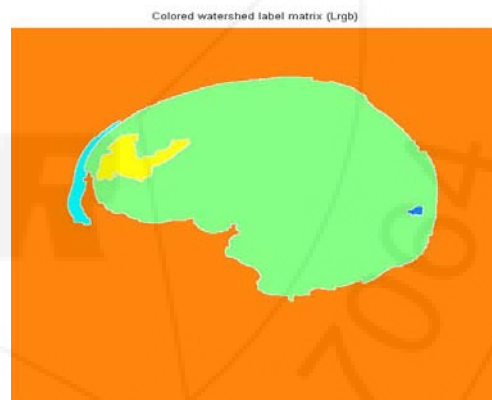


Figure 13: Segmented brain tissues (a) colored watersheded label matrix (b) `Lrgb` superimposed transparently on original image

4. Conclusion

This experimental study was conducted to study an accurate brain tissues segmentation method using a parallel computing algorithm in MRI images. In addition to evaluate the usage of new nonlinear approach for contrast enhancement of soft tissues in MRI images in order to study automatic extraction of brain. In image processing, filters are mainly used to suppress either the high frequencies in the image, i.e. smoothing the images or the low frequencies, i.e. enhancing or detecting edges in the image. Due to various factors the images are in general poor in contrast. Researchers applied image pre-processing to remove artefacts and degradations such as blurring and noise. A variety of smoothing filters have been developed that are not linear. While they cannot, in general, be submitted to Fourier analysis, their properties and domains of application have been studied extensively. For this reason researchers applied anisotropic filtering and median filtering. In study method anisotropic and median filtering algorithms were used.

References

- [1] Abdallah YMY. Wagiallah EW. 2014. Segmentation of Thyroid Scintigraphy Using Edge Detection and Morphology Filters, International Journal of Science and Research. Volume 3, Issue 11, pp.2768-2771
- [2] Abdallah YMY. Wagiallah EW. 2014. Enhancement of Nuclear Medicine Images using Filtering Technique, International Journal of Science and Research. Volume 3, Issue 8, pp.916-921
- [3] Wagiallah EW. Ahmed Y. Abdallah YMY. 2014. Correction Preprocessing Method for Cardiac Scintigraphy Images using Local Adaptive Filters, International Journal of Science and Research. Volume 3, Issue 8, pp.1885-1889
- [4] Abdallah YMY. Abdelwahab RI. 2014. Application of Texture Analysis Algorithm for Data Extraction in Dental X-Ray Images, International Journal of Science and Research. Volume 3, Issue 8, pp.1934-1937
- [5] Adam MJ, Wilbur DS .2005. Radiohalogens for imaging and therapy. Chem Soc Rev 34:153-63
- [6] Adelson, E.H., Bergen, J.R. 1991. "The plenoptic function and the elements of early vision", In Computation Models of Visual Processing, M. Landy and J.A. Movshon, eds., MIT Press, Cambridge, 1991, pp. 3-20.
- [7] Arvo, J., 1994, The Irradiance Jacobian for Partially Occluded Polyhedral Sources, Proc. ACM SIGGRAPH, ACM Press, pp. 335-342.
- [8] Ball, J., Moore, A., 1997, Essential physics for radiographers, 3rd edition, Blackwell Scientific, Oxford.
- [9] Ball, J., Price, T., 1995, Chesney's radiographic imaging, 6th edition, Blackwell Scientific, Oxford.
- [10] Buehler, C., Bosse, M., McMillan, L., Gortler, S., Cohen, M., 2001, Unstructured Lumigraph rendering, Proc. ACM SIGGRAPH, ACM Press.
- [11] Farr, R., Allisy-Roberts, P., 1997, Physics for medical imaging, W.B. Saunders, London.
- [12] Fritsch D.S.; Chaney E.L.; McAuliffe M.J.; Raghavan S.; Boxwala A.; Earnhart J.R.D., 1995, International

Journal of Radiation Oncology, Biology, Physics, Volume 32, Number 971, , pp. 217-217.

- [13] Georgiev, T., Zheng, C., Nayar, S., Curless, B., Salesin, D., Intwala, C., 2006, Spatio-angular Resolution Trade-offs in Integral Photography, Proc. EGSR .

Author Profile



Yousif Mohamed Yousif Abdallah received the B.S., M.Sc. and PhD degrees and M.Sc. in nuclear medicine and Radiotherapy Technology from College of Medical radiological Science, Sudan University of Science and Technology in 2005, 2009 and 2013, 2014, respectively. During 2006 up to date, he is staying in College of Medical radiological Science, Sudan University of Science and Technology. He is now assistant professor, college registrar and Consultant Radiation Therapist.



Abdalrahman Hassan received the B.S. in radiotherapy technology from College of Medical radiological Science, Sudan University of Science and Technology in 2013. During 2013 up to date, he is staying in College of Medical radiological Science, Sudan University of Science and Technology and Radiology Department, Antalia Medical Center.